

Kinetics of nickel extraction from Indonesian saprolitic ore by citric acid leaching under atmospheric pressure

W. Astuti

Graduate student, Department of Earth Resources Engineering, Faculty of Engineering, Kyushu University, Fukuoka, Japan and researcher, Mineral Processing Division, Indonesian Institute of Sciences (LIPI), Indonesia

T. Hirajima*, K. Sasaki and N. Okibe

Professor, professor and associate professor, respectively, Department of Earth Resources Engineering, Faculty of Engineering, Kyushu University, Fukuoka, Japan

*Corresponding author email: hirajima@mine.kyushu-u.ac.jp

Abstract

The kinetics of leaching of a saprolitic ore from Indonesia by citric acid solution under atmospheric pressure was investigated. An examination of the effects of leaching temperature, citric acid concentration, pulp density and ore particle size on the dissolution rate of nickel found that they all had significant influence on the rate. The highest nickel recovery (95.6 percent) was achieved under the leaching conditions of ore particle size of 212-355 microns, citric acid concentration of 1 M, leaching time of 15 days, pulp density of 20 weight/volume percent, leaching temperature of 40°C and shaker speed of 200 rpm. The shrinking core model was found to be appropriate for describing the leaching kinetics of this ore in citric acid solutions at atmospheric pressure. The experimental data were well interpreted by this model with rate of reaction controlled by diffusion through the solid product layer. Using the Arrhenius expression, the apparent activation energy for nickel dissolution was evaluated as 12.38 kJ/mol. Finally, on the basis of the shrinking core model, a proposed empirical kinetic model for the leaching of nickel from this Indonesian saprolitic ore was expressed as a mathematical model, which was verified as consistent with the observed experimental results.

Minerals & Metallurgical Processing, 2015, Vol. 32, No. 3, pp. 176-185.

An official publication of the Society for Mining, Metallurgy & Exploration Inc.

Key words: Leaching, Kinetics, Nickel extraction, Saprolitic ore, Citric acid, Shrinking core model

Introduction

Indonesia has some of the world's largest nickel laterite reserves and was the largest producer of nickel – in the form of nickel lateritic ores – in the world in 2013 (Merchant Research and Consulting Ltd, 2014). However, only high-grade saprolites are processed in Indonesia using pyrometallurgical methods to produce ferronickel and nickel matte. Lower-grade saprolites and limonites are removed, becoming waste or overburden in mining site areas. Hydrometallurgical methods, involving either chemical leaching or bioleaching, are now seen as the most important technologies for treating nickel laterites in the future because of their advantage of not only extracting nickel and iron but also other valuable elements. In addition, hydrometallurgical methods consume less energy and have lower capital and operational costs. Although they are recognized to be more suited to limonites, some researchers have studied their use in the extraction of nickel and other metals from saprolites (Guo et al., 2009; Lu et al., 2013). Hydrometallurgical processes

for the extraction of metals, especially nickel, promise to be meaningful alternatives to pyrometallurgical processes to primarily treat low-grade saprolites for which pyrometallurgical processing is not favorable.

Various hydrometallurgical methods for the leaching of saprolitic ores from Indonesia at atmospheric pressure have been reported. Sufriadin et al. (2011) reported that chemical leaching using sulfuric acid (25 weight percent) at 90°C under atmospheric conditions to recover nickel and other metals from the saprolitic nickel ores of Sorowako (Sulawesi Island) achieved nickel recovery of about 58 percent after three hours. Fan and Gerson (2013) dissolved saprolitic ores from Raja Ampat, West Papua, in sulfuric acid (98 weight percent) in conditions of 25 percent pulp density, 100°C and atmospheric pressure for 11 hours and reported nickel extraction of greater than 80 percent. For environmental reasons, Mubarak et al. (2011) investigated the use of organic acids including citric, lactic, acetic and oxalic acids for the leaching of nickel from an Indonesian saprolite and found that citric acid gave the best nickel recovery. Many other researchers had confirmed that citric acid performs most effectively in the leaching of nickel laterites compared with

Paper number MMP-14-053. Original manuscript submitted June 2014. Revised manuscript accepted for publication November 2014. Discussion of this peer-reviewed and approved paper is invited and must be submitted to SME Publications Dept. prior to Feb. 29, 2016. Copyright 2015, Society for Mining, Metallurgy & Exploration Inc.

Table 1 – Chemical analysis of raw materials by X-ray diffraction (mass percentage).

| Constituents | SiO ₂ | Fe | Ni | Co | Mg | Mn | Cr | Al |
|--------------------------|------------------|-------|------|------|------|------|------|------|
| Content (weight percent) | 36.30 | 21.64 | 1.76 | 0.06 | 8.44 | 0.43 | 1.07 | 2.04 |

Table 2 – Atomic percentages (determined by EDS) of the raw material particles shown in Fig. 2.

| | O | Fe | Mg | Ni | Si | Al | Mineral type |
|---|-------|-------|-------|------|------|------|--------------|
| 1 | 58.14 | 9.78 | 16.49 | 3.25 | 7.09 | 0.00 | Serpentine |
| 2 | 55.09 | 13.70 | 14.42 | 4.02 | 7.70 | 0.79 | Serpentine |
| 3 | 47.64 | 32.02 | 5.43 | 1.20 | 5.87 | 0.00 | Goethite |
| 4 | 47.32 | 33.05 | 4.17 | 2.93 | 4.64 | 1.16 | Goethite |

other organic acids (Tzeferis and Agatzini-Leonardou, 1994; Tang and Valix, 2006; McDonald and Whittington, 2008). Tzeferis and Agatzini-Leonardou (1994) compared the abilities of citric, lactic, oxalic, acetic, formic and salicylic acids to solubilize nickel and iron from two types of Greek laterites comprising low-grade hematitic laterite and garnieritic ores. Tang and Valix (2006) studied the effect of acid activity, type of organic acid (citric, lactic and malic acids), and pulp density on nickel and cobalt dissolution and the leaching selectivity of New Caledonian limonitic and nontronitic ores. McDonald and Whittington (2008) reviewed studies of atmospheric acid leaching of nickel laterites by both chemical leaching, using inorganic and organic acids, and bioleaching. Although citric acid needs more leaching time compared with inorganic acids, it offers not only high nickel recovery and high selectivity of leaching (Mubarok et al., 2011) but also an environmentally safe process and low acid consumption. In addition, citric acid can be produced from fungal metabolism using several types of carbon sources as fungal nutrients. The use of citric acid for nickel extraction from Indonesian laterites can therefore be considered a potentially suitable alternative technology that will

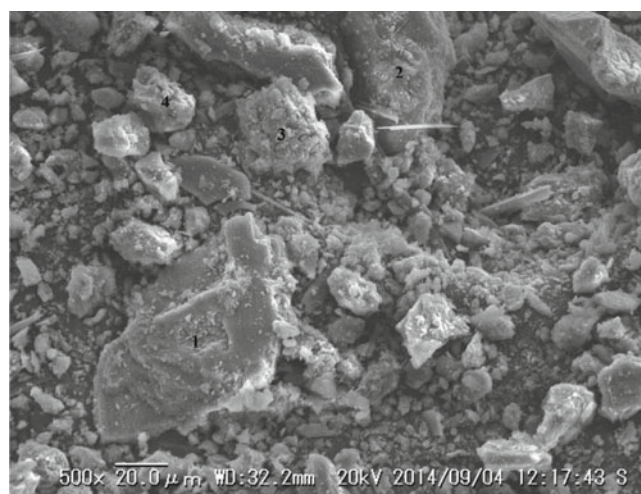


Figure 2 – SEM images of selected raw saprolitic nickel-containing grains. EDS analysis (Table 2) suggests the nickel is probably associated with serpentine and goethite.

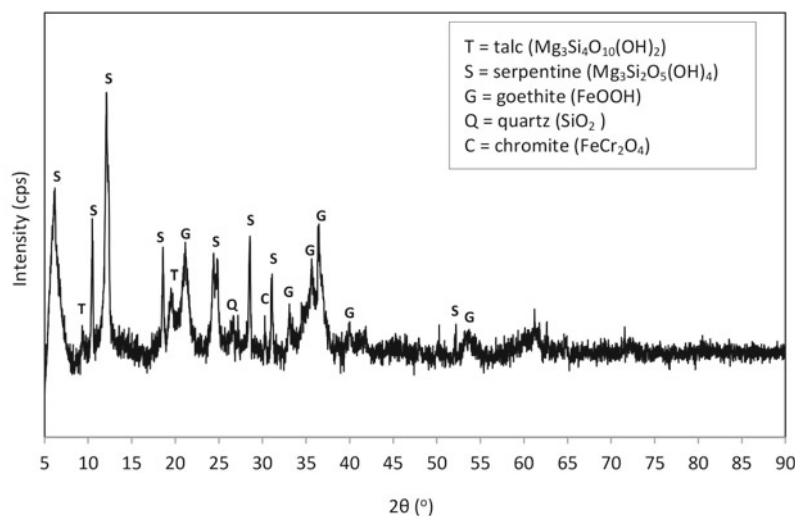


Figure 1 – X-ray diffraction pattern of the raw saprolitic ore.

entail low capital and operational costs owing to the country's abundance of biodiversity and carbon sources.

Previous work had only observed the effects of different organic acids on nickel recovery and leaching selectivity. The effects of leaching parameters such as particle size, pulp density, acid concentration and leaching temperature on nickel leaching behavior and kinetics, especially for saprolite processing, had not been studied. The present study therefore investigates the effects of various leaching parameters on the leaching of a saprolite from Sulawesi Island, Indonesia, by citric acid solution at atmospheric pressure. Kinetic measurements were modeled and used to identify the rate-determining step of the leaching process and to calculate the kinetic parameters.

Materials and methods

Materials. Saprolitic ore was collected from a mining site on Sulawesi Island. The sample was mineralogically and chemically characterized. X-ray fluorescence (XRF) and inductively coupled plasma-optical emission spectroscopy (ICP-OES) were used to determine the chemical composition. The sample was found to have high magnesium, silica and nickel contents (Table 1). The mineral phases of the sample were determined using X-ray diffraction (XRD) with Cu K α radiation between 5° and 80° 2 θ . Serpentine (Mg₃Si₂O₅(OH)₄) and goethite (FeOOH) were the predominant minerals (Fig. 1). Scanning electron microscopy combined with energy-dispersive X-ray spectroscopy (SEM/EDS) was also used to determine the nickel content of the different minerals. Typical SEM/EDS results

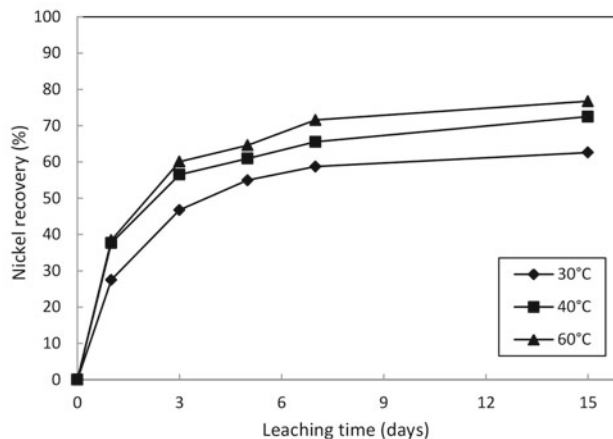


Figure 3 — Effect of leaching temperature on nickel recovery (1 M citric acid, 5 w/v percent pulp density, < 75 microns particle size, 200 rpm shaker speed).

(Fig. 2 and Table 2) confirm the presence of nickel-containing serpentine and goethite.

Chemical leaching procedures. Chemical leaching experiments were performed using a 300-mL flask placed in a mechanical shaker with 200-rpm shaker speed at atmospheric pressure. Analytically pure citric acid was used as the leach-

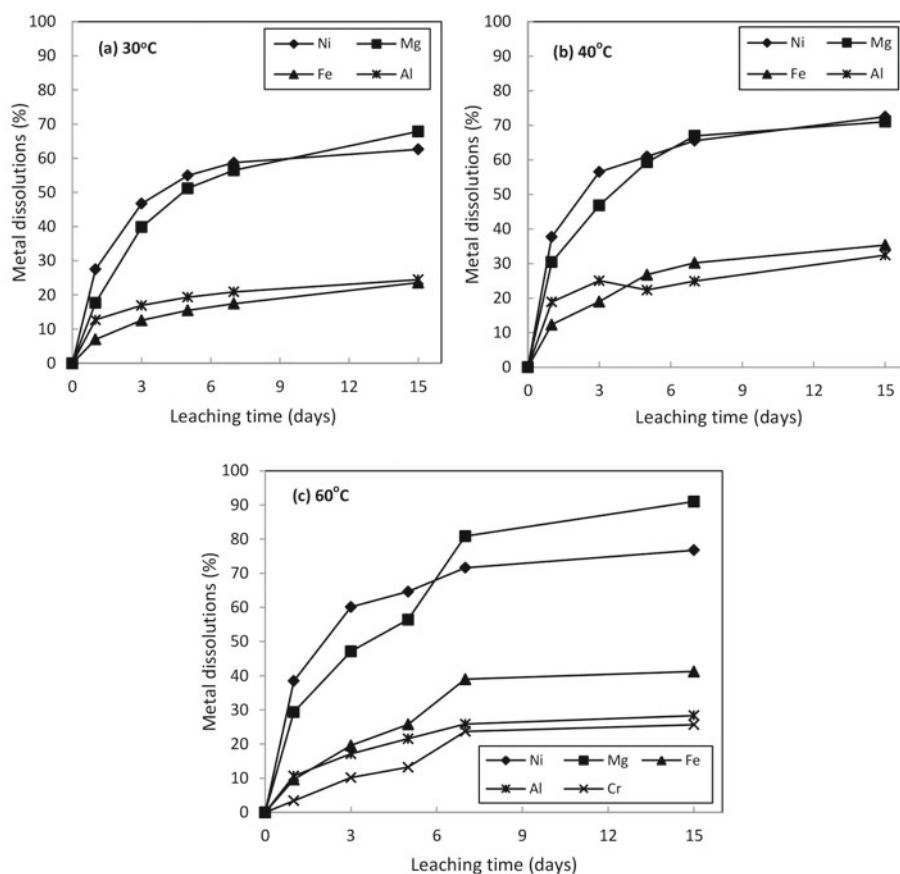


Figure 4 — Effect of leaching temperature on metal dissolutions: (a) 30°C (b) 40°C and (c) 60°C (1 M citric acid, 5 w/v percent pulp density, < 75 microns particle size, 200 rpm shaker speed).

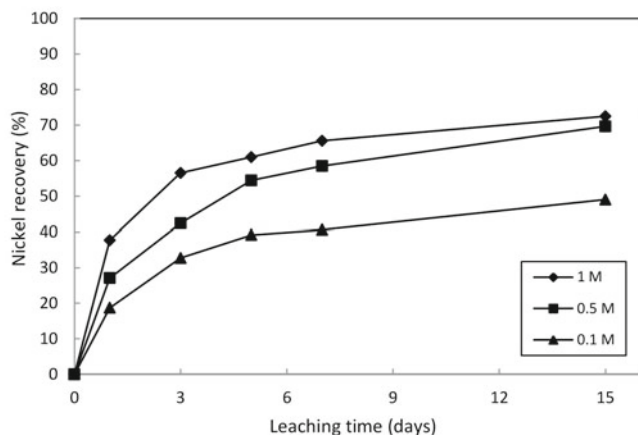


Figure 5 — Effect of citric acid concentration on nickel recovery (40°C, 5 w/v percent pulp density, < 75 microns particle size, 200 rpm shaker speed).

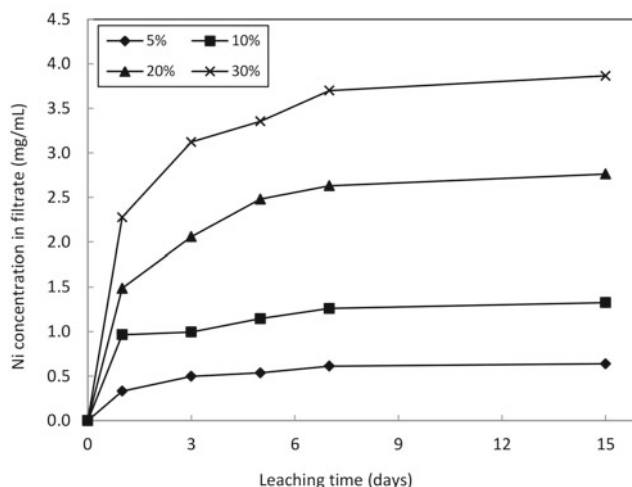


Figure 6 — Nickel concentration in the filtrate for various pulp densities (1 M citric acid, 40°C, < 75 microns particle size, 200 rpm shaker speed).

ing agent. Solution samples were periodically withdrawn for pH measurement and chemical analyses for nickel and other elements by ICP-OES using standard procedures.

The kinetic analysis was performed based on experimental data for the dissolution of nickel. Kinetic experiments were carried out under the following reaction conditions: leaching temperatures of 30°C, 40°C and 60°C; citric acid concentrations of 0.1, 0.5 and 1 M; shaking speed of 200 rpm; pulp densities of 5, 10, 20 and 30 weight/volume (w/v) percent; and ore particle sizes of < 75, 75-150, 212-355 and 355-850 microns.

Results and discussion

Effect of leaching temperature on nickel extraction.

Leaching temperature is a significant parameter influencing nickel extraction. The leaching tests were carried out with 1 M citric acid, 5 w/v percent pulp density, ore particle size of < 75 microns and 200-rpm shaker speed at three different leaching temperatures (30°C, 40°C and 60°C). The results, shown in Fig. 3, indicate that temperature has an appreciable effect on nickel extraction. The maximum nickel recovery rate increased from 62.6 percent at 30°C to 72.5 percent at 40°C after 15 days of leaching. However, nickel recovery was not strongly influenced on further raising the temperature: nickel recovery rose slightly from 72.5 percent at 40°C to 76.7 percent at 60°C. Moreover, the leaching selectivity of nickel over other metals at 60°C was lower than at 40°C (Fig. 4). In addition, Fig. 4(c) shows that chromium (Cr) starts leaching at 60°C. Because the presence of Cr in the filtrate is detrimental to downstream nickel recovery processes, 40°C was selected as the optimum leaching temperature in this study, and this value was used in subsequent experiments.

These experiments also showed that a longer leaching time leads to higher nickel recovery, up to an optimum value. Nickel dissolution increased rapidly during the first seven days but slowed down between Day 7 and 15. The leaching process was essentially complete after 15 days, when no further nickel dissolution occurred.

Effect of citric acid concentration on nickel extraction.

Citric acid concentration is also a significant parameter influencing nickel extraction. The effects of citric acid on the nickel recovery were studied for concentrations of 0.1, 0.5 and 1 M at

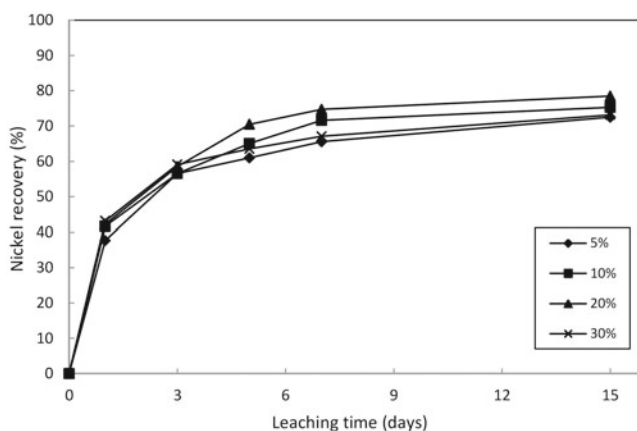


Figure 7 — Effect of pulp density on nickel recovery (1 M citric acid, 40°C, < 75 microns particle size, 200 rpm shaker speed).

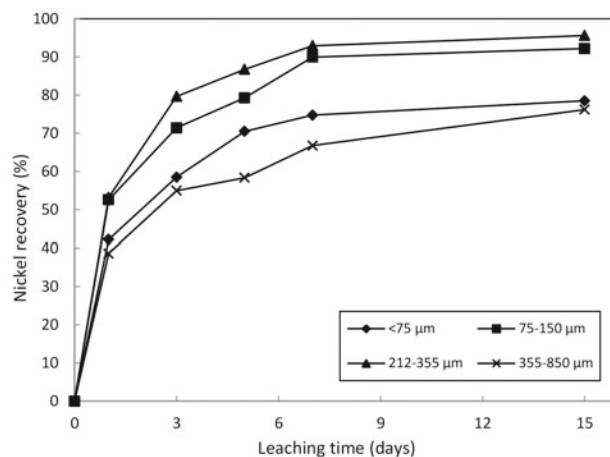


Figure 8 — Effect of ore particle size on nickel recovery (1 M citric acid, 40°C, 20 w/v percent pulp density, 200 rpm shaker speed).

Table 3 — Correlation coefficients (R^2) of the kinetic models for various experimental parameters.

| Experimental parameters | Shrinking core model | | | Shrinking particle model | | |
|----------------------------------|------------------------------|---------------------------|---------------------------------|------------------------------|---------------------------|--------|
| | Fluid film diffusion control | Chemical reaction control | Product layer diffusion control | Fluid film diffusion control | Chemical reaction control | |
| Temperature effect | 30°C | 0.8264 | 0.8780 | 0.9712 | 0.8529 | 0.8780 |
| | 40°C | 0.7402 | 0.8102 | 0.9328 | 0.7754 | 0.8102 |
| | 60°C | 0.7701 | 0.8504 | 0.9575 | 0.8109 | 0.8504 |
| Citric acid concentration effect | 1 M | 0.7402 | 0.8102 | 0.9328 | 0.7754 | 0.8102 |
| | 0.5 M | 0.8578 | 0.9082 | 0.9866 | 0.8841 | 0.9082 |
| | 0.1 M | 0.8236 | 0.8525 | 0.9476 | 0.8383 | 0.8525 |
| Pulp density effect | 5% | 0.7402 | 0.8743 | 0.9328 | 0.7754 | 0.8743 |
| | 10% | 0.7661 | 0.8566 | 0.9772 | 0.8121 | 0.8566 |
| | 20% | 0.7813 | 0.8102 | 0.9790 | 0.8292 | 0.8102 |
| | 30% | 0.6898 | 0.7656 | 0.9032 | 0.7275 | 0.7656 |
| Ore particle size effect | <75 microns | 0.7813 | 0.8743 | 0.9772 | 0.8292 | 0.8743 |
| | 75–150 microns | 0.7597 | 0.9066 | 0.9845 | 0.8369 | 0.9066 |
| | 212–355 microns | 0.7443 | 0.9016 | 0.9749 | 0.8244 | 0.9016 |
| | 355–850 microns | 0.7495 | 0.8263 | 0.9536 | 0.7883 | 0.8263 |

40°C, 200-rpm shaker speed and atmospheric pressure using ore particle size of < 75 microns and pulp density of 5 w/v percent. Figure 5 shows that nickel dissolution and leaching rate are strongly dependent on the citric acid concentration. The citric acid concentration could be increased to a certain limit. At low acid concentration of 0.1 M, there was an acid deficiency and only 49.0 percent of the nickel was extracted after 15 days. Nickel extraction increased to 69.6 percent and 72.5 percent when the citric acid concentration was increased to 0.5 M and 1 M, respectively. This effect is attributed to an increase in hydronium ion (H^+) activity with increasing acid concentration, which leads to the further dissolution of nickel-containing material.

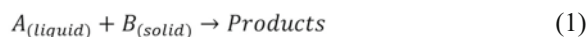
Effect of pulp density on nickel extraction. The influences of pulp densities at 5, 10, 20 and 30 w/v percent on nickel recovery were also examined, with the other parameters kept constant at citric acid concentration of 1 M, ore particle

size of < 75 microns, temperature of 40°C and shaker speed of 200 rpm. Figure 6 shows that the nickel concentration in the filtrate increased sharply with increasing pulp density. However, when nickel recoveries were calculated (Fig. 7), it was found that after 15 days nickel recovery rose only slightly from 72.5 percent at pulp density of 5 w/v percent to 75.3 and 78.5 percent at pulp densities of 10 and 20 w/v percent, respectively, and then decreased to 73.2 percent at pulp density of 30 w/v percent. From these results, it was recognized that a moderate pulp density of 20 w/v percent was adequate in the current study. This value was used in all subsequent leaching tests.

Effect of ore particle size on nickel extraction. The effect of ore particle size on nickel recovery was studied for four different size ranges: <75, 75-150, 212-355 and 355-850 microns. All experiments were conducted at 40°C, 200-rpm shaker speed and atmospheric pressure using citric acid concentration of 1 M

and pulp density of 20 percent. Figure 8 shows that increasing particle size led to increased nickel recovery up to 212-355 microns. This particle size range yielded the maximum nickel recovery (95.6 percent), followed by the particle size ranges of 75-150, < 75 and 355-850 microns, which produced 92.2, 78.5 and 76.2 percent nickel recovery, respectively, after 15 days of leaching. The optimum particle size range was selected as 212-355 microns.

Kinetic analysis of nickel extraction. The leaching of saprolite is a solid-liquid reaction. In such a reaction system, soluble reactants diffuse across the interface and/or through a porous solid layer and then the chemical reactions occur. The leaching rate is generally controlled by the (1) diffusion through the fluid film, (2) diffusion through the solid product layer on the particle surface and/or (3) chemical reaction at the surface of the unreacted core/particle. The rate of the process is controlled by the slowest of these sequential steps (Levenspiel, 1999). The reaction model between solid and liquid may be given as follows:



Depending on the parameter conditions and type and nature of the solid materials and leaching reagent, different reaction mechanisms and kinetics have been suggested (Gharabaghi et al., 2010). To analyze the kinetics of nickel dissolution, this study used two types of solid-liquid kinetic models proposed by Levenspiel (1999): the shrinking-core model (SCM) and the shrinking-particle model (SPM). In the SCM, the three possible rate-determining steps detailed above are applied in the kinetic analysis. In the SPM, there are only two possible rate-determining steps: diffusion through the fluid film and chemical reaction at the surface of the unreacted particles (Levenspiel, 1999).

The SCM equations for the three rate-determining steps can be written as follows (Levenspiel, 1999):

Fluid film diffusion control:

$$x = k_f t = k \exp\left(-\frac{E_a}{RT}\right) t \quad (2)$$

Diffusion through solid product layer control:

$$1 - 3(1-x)^{\frac{2}{3}} + 2(1-x) = k_d t = k \exp\left(-\frac{E_a}{RT}\right) t \quad (3)$$

Chemical reaction control:

$$1 - (1-x)^{\frac{1}{3}} = k_r t = k \exp\left(-\frac{E_a}{RT}\right) t \quad (4)$$

The following are the mathematical model equations for the SPM (Levenspiel, 1999):

Fluid film diffusion control:

$$1 - (1-x)^{\frac{2}{3}} = k_f t = k \exp\left(-\frac{E_a}{RT}\right) t \quad (5)$$

Chemical reaction control:

$$1 - (1-x)^{\frac{1}{3}} = k_r t = k \exp\left(-\frac{E_a}{RT}\right) t \quad (6)$$

where x is the fraction reacted, k is the overall reaction rate constant in min^{-1} , A is the frequency factor in min^{-1} , E_a is the apparent activation energy in Jmol^{-1} , R is the universal gas constant ($8.314 \text{ JK}^{-1}\text{mol}^{-1}$), T is the reaction temperature in K, t is the leaching time in days, and k_f , k_d and k_r are the rate constants (Levenspiel, 1999).

The kinetics of nickel extraction was studied using these two models based on the experimental data. The left-hand sides of Eqs. (2)-(6) were plotted with respect to leaching time and the dependencies of these models on the kinetic data were evaluated using the correlation coefficient (R^2) values. The slopes of these plots give the apparent rate constants (k_f , k_d and k_r).

The R^2 values are presented in Table 3. This detailed kinetic

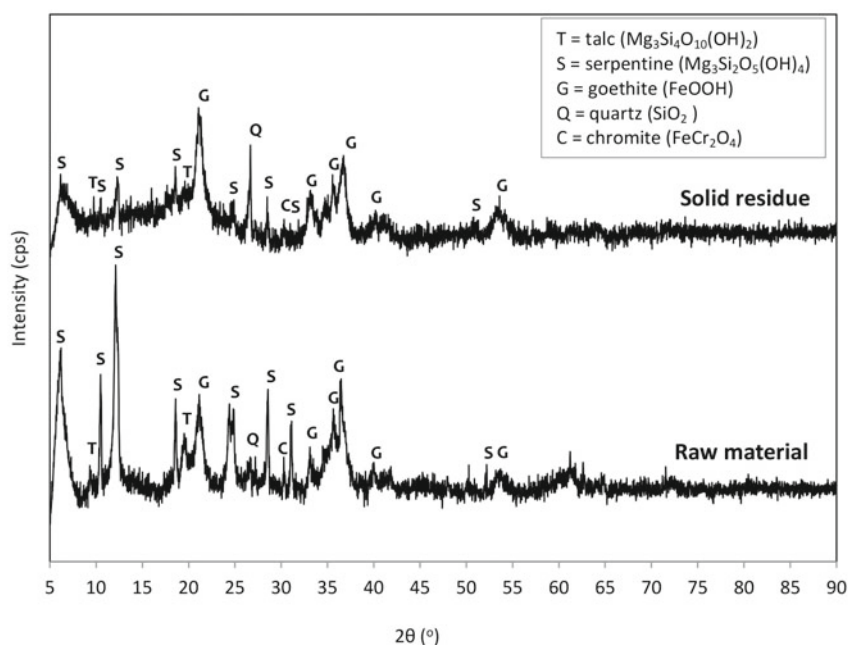


Figure 9 — X-ray diffraction pattern of solid residue after leaching for 15 days under the best conditions (1 M citric acid, 212-355 microns particle size, 40°C, 20 w/v percent pulp density, 200 rpm shaker speed).

evaluation shows that the SCM with diffusion through the solid product layer gave the highest R^2 value for all experimental data considered. It is therefore concluded that the SCM is the most appropriate kinetic model for this system and that diffusion through the solid product layer is the step that controls the rate of leaching under the experimental conditions.

Nickel in this saprolite is mostly incorporated in serpentine, according to the XRD (Fig. 1) and SEM/EDS analyses (Fig. 2 and Table 2). After 15 days of leaching, XRD of the solid residue (Fig. 9) showed decreased intensities of the serpentine peaks while the peaks of other minerals increased. It can therefore be assumed that most of the dissolved nickel originated from serpentine. Metal ion dissolution from ser-

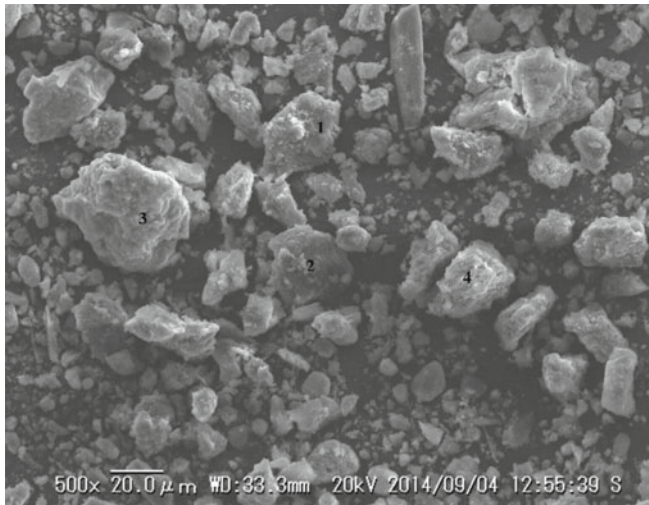


Figure 10 – SEM images of selected solid residue nickel-containing grains after 15 days of leaching under the best conditions (1 M citric acid, 212-355 microns particle size, 40°C, 20 w/v percent pulp density, 200 rpm shaker speed).

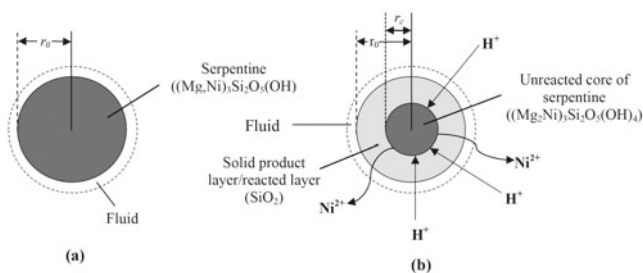
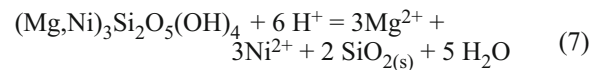
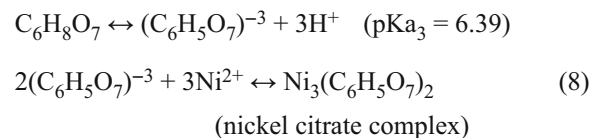


Figure 11 – Schematic of the nickel leaching process from serpentine based on the SCM: (a) initial state and (b) state at time t .

pentine can be described as follows:



H^+ is provided by the dissociation of citric acid. Two mechanisms are proposed for metal dissolution by citric acid: (1) acid attack and displacement of metal ions by hydrogen ions and (2) chelation of metals to form soluble metal–ligand complexes (McDonald and Whittington, 2008). Citric acid contains three carboxyl groups. When this acid is fully dissociated, the possible complexes of the nickel cation with a citrate anion are expressed as (Behera et al., 2011):



Silica (SiO_2) from the reaction in Eq. (7) will become the product layer in the solid residue. It can be seen from SEM/EDS analyses of the solid residue (Fig. 10 and Table 4) that silica in serpentine remains in the solid residue. These data are interpreted as indicating that there is not only pore diffusion but also chemical reaction occurring at the solid surface, as in the SCM. A schematic of nickel dissolution from serpentine according to the SCM is illustrated in Fig. 11, where serpentine is represented as the nonporous solids. The chemical reaction between the leaching agent, that is, citric acid, and nickel occurs at the serpentine surface, dissolving nickel and magnesium. Silica remains in the reacted layer, as presented in Eq. (7), and the reacted layer becomes porous. The next step is the penetration and diffusion of citric acid through the reacted layer to the surface of the unreacted core, and chemical reaction will occur at the surface of the unreacted core. Finally, the dissolved product diffuses through the solid reacted layer back to the exterior surface of the solid and into the main bulk of the fluid.

The apparent activation energy was calculated based on the Arrhenius equation:

$$k_d = A \exp\left(-\frac{E_a}{RT}\right) \quad (9a)$$

$$\ln k_d = \ln A - \frac{E_a}{RT} \quad (9b)$$

Arrhenius plots of $\ln k_d$ (the apparent rate constant for control by diffusion through the solid product layer for the SCM) against $1000/T$ for the experimental data are shown in Fig. 12 and Table 5. The apparent activation energy determined for nickel extraction from this Indonesian saprolite using citric acid at atmospheric pressure was 12.38 kJ/mol. This low activation energy is appropriate for a process that is controlled by the diffusion through a solid product layer and provides further confirmation of the importance of diffusion through a product layer as the kinetic-limiting step (Veglio et al., 2001).

Table 4 – Atomic percentages (determined by EDS) of the solid residue particles shown in Fig. 10.

| | O | Fe | Mg | Ni | Si | Al | Mineral type |
|---|-------|-------|-------|------|------|------|--------------|
| 1 | 59.37 | 9.37 | 11.26 | 0.93 | 8.38 | 1.79 | Serpentine |
| 2 | 63.66 | 5.00 | 11.96 | 1.11 | 8.92 | 0.00 | Serpentine |
| 3 | 52.48 | 24.24 | 7.85 | 2.20 | 7.47 | 0.80 | Goethite |
| 4 | 48.27 | 19.47 | 7.02 | 2.77 | 5.73 | 0.63 | Goethite |

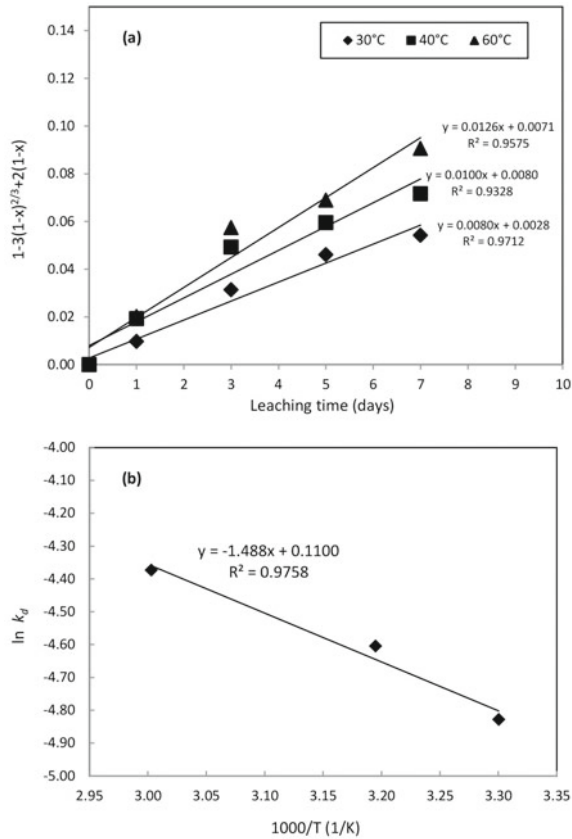


Figure 12 — (a) Plot of diffusion through the solid product layer for the SCM with leaching time at various temperatures (b) Arrhenius plot for nickel leaching (1 M citric acid, 5 w/v percent pulp density, < 75 microns particle size, 200 rpm shaker speed).

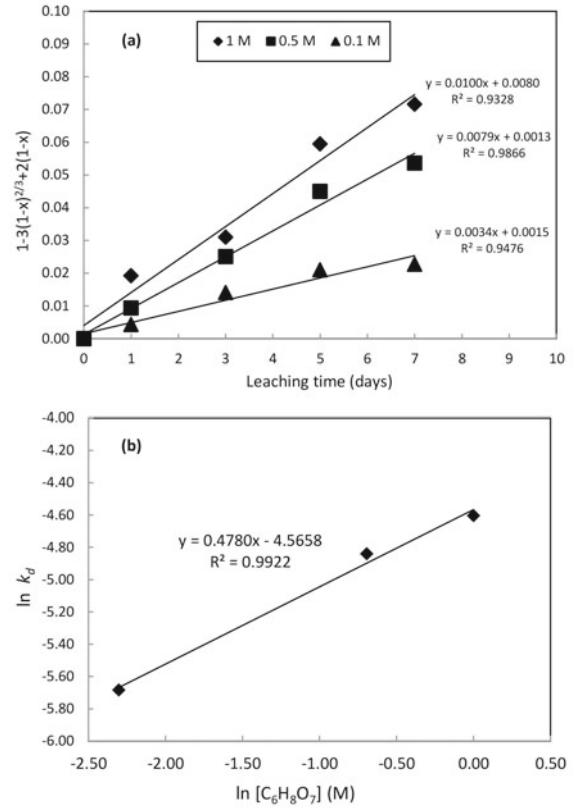


Figure 13 — (a) Plot of diffusion through the solid product layer for the SCM with leaching time at various citric acid concentrations (b) Plot of $\ln k_d$ versus $\ln [C_6H_8O_7]$ (40°C, 5 w/v percent pulp density, < 75 microns particle size, 200 rpm shaker speed).

Previously reported low values (< 24 kJ/mol) for the activation energy of diffusion-controlled reactions are: 4-12 kJ/mol (Hou et al., 2010; Habashi, 1969), 8-20 kJ/mol (Liu et al., 2012) and 12-24 kJ/mol (Romankiw and Bruyn, 1964). In contrast, a leaching process controlled by a surface chemical reaction has higher activation energies: 40-80 kJ/mol (Habashi, 1969; Sohn and Wadsworth, 1979; Luo et al., 2010).

The current work also found that the kinetic behavior of citric acid leaching differs from that of sulfuric acid leaching under atmospheric conditions. Luo et al. (2010) analyzed the kinetics of saprolite leaching by sulfuric acid and reported that the chemical reaction is the rate-determining step. However, in the current work using citric acid, it is found that diffusion through the solid product layer is rate limiting. A diffusion-controlled process is usually slightly dependent on temperature while a chemically controlled process is very sensitive to temperature (Habashi, 1969; Sohn and Wadsworth, 1979). These experiments show that citric acid leaching can produce high nickel recoveries at lower temperature and atmospheric conditions. The optimum nickel recovery achieved in this study was 95.6 percent at 40°C. Previous work on the sulfuric acid leaching of saprolitic ore under atmospheric pressure only produced maximum nickel recoveries of 84.8 (Luo et al., 2010) and 58 percent (Sufriadin et al., 2011), respectively, at 90°C leaching temperature.

Similar plots of $1 - 3(1 - x)^{2/3} + 2(1 - x)$ as a function of leaching time were obtained for different citric acid concentrations $[C_6H_8O_7]$, solid-liquid ratios (or pulp densities) (S/L),

Table 5 — Reaction rate constants at various temperatures.

| T (°C) | T (K) | 1000/T (1/K) | k_d | $\ln k_d$ |
|-------------------|-------|--------------|--------------|-----------|
| 30 | 303 | 3.3003 | 0.0080 | -4.828 |
| 40 | 313 | 3.1949 | 0.0100 | -4.605 |
| 60 | 333 | 3.0030 | 0.0126 | -4.374 |
| Activation energy | | | 12.38 kJ/mol | |

and ore particle sizes (r_0) (Figs. 13a, 14a and 15a). These control factors were used to formulate the kinetic model. The relationship between the apparent rate constant of diffusion through the solid product (k_d) and these factors is given by:

$$k_d = k_0 [C_6H_8O_7]^a (S/L)^b (r_0)^c e^{-\frac{E_a}{RT}} \quad (10)$$

Hence, the total kinetic model from Eqs. (4) and (10) is obtained as:

$$1 - 3(1 - x)^{2/3} + 2(1 - x) = k_d t = k_0 [C_6H_8O_7]^a (S/L)^b (r_0)^c e^{-\frac{E_a}{RT}} t$$

where k_0 is the Arrhenius constant, which can be calculated

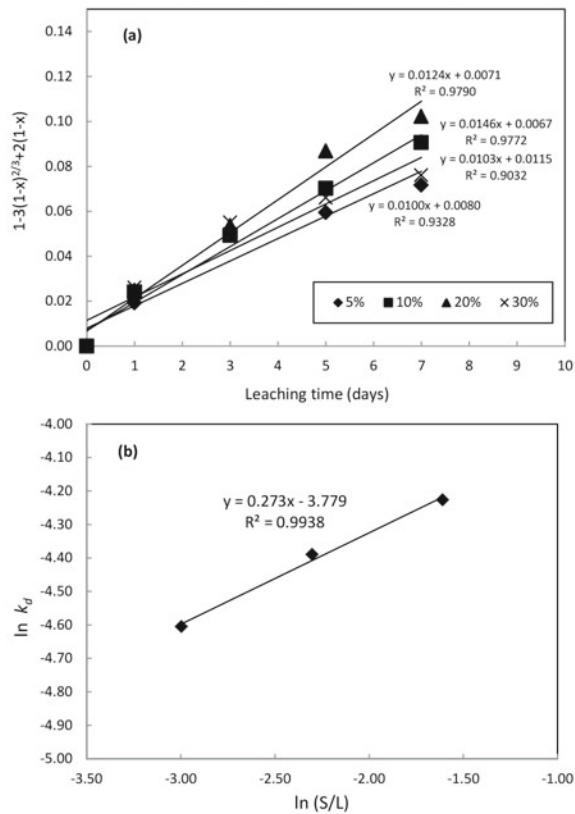


Figure 14 — (a) Plot of diffusion through the solid product layer for the SCM with leaching time at various pulp densities (b) Plot of $\ln k_d$ versus $\ln(S/L)$ (40°C, 1 M citric acid, < 75 microns particle size, 200 rpm shaker speed).

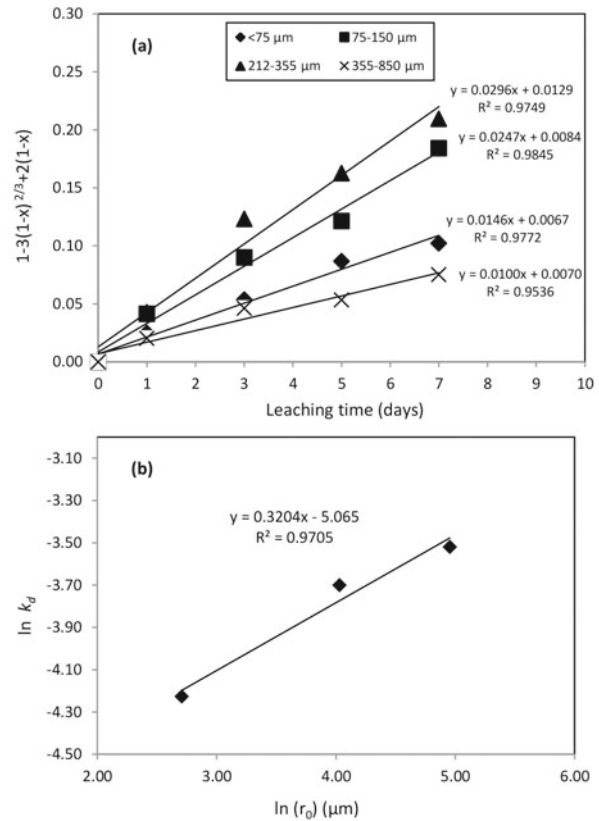


Figure 15 — (a) Plot of diffusion through the solid product layer for the SCM with leaching time at various ore particle sizes (b) Plot of $\ln k_d$ versus $\ln(r_0)$ (40°C, 20 w/v percent pulp density, 1 M citric acid, 200 rpm shaker speed).

from the intercept of the straight line in Fig. 12.

The apparent rate constant (k_d) values were determined from the slopes of the straight lines. Plots of $\ln(k_d)$ against $\ln[C_6H_8O_7]$, $\ln(S/L)$ and $\ln(r_0)$ (Figs. 13b, 14b and 15b, respectively) were established to calculate the empirical orders of dependency with respect to citric acid concentration, pulp density and ore particle size as 0.48, 0.27 and 0.32, respectively. The Arrhenius equation obtained from Fig. 10 is:

$$\ln k_d = 0.1100 - \frac{1488}{T}. \text{ Thus,}$$

$$k_0 [C_6H_8O_7]^{0.48} (S/L)^{0.27} (r_0)^{0.32} = \exp(0.1100) = 1.1163$$

Substituting $[C_6H_8O_7] = 1$ M, $S/L = 0.05$ w/v percent and $r_0 = 15$ microns gives $k_0 = 7.32 \times 10^{-4} \text{ min}^{-1}$. Therefore, the empirical kinetic model for nickel extraction from this Indonesian saprolite by citric acid leaching under atmospheric pressure is:

$$k_d t = 1 - 3(1-x)^{\frac{2}{3}} + 2(1-x) = 7.32 \times 10^{-4} [C_6H_8O_7]^{0.48} (S/L)^{0.27} (r_0)^{0.32} e^{-\frac{12,380}{RT}} t$$

To validate this empirical kinetic model, the values of

$1 - 3(1-x)^{\frac{2}{3}} + 2(1-x)$ at selected leaching conditions of temperature, citric acid concentration, pulp density and particle size were calculated from the empirical mathematical model. The plots of $[1 - 3(1-x)^{\frac{2}{3}} + 2(1-x)]_{\text{equation}}$ against $[1 - 3(1-x)^{\frac{2}{3}} + 2(1-x)]_{\text{experimental}}$ for some experimental

data in Fig. 16 show good correlation between the empirical kinetic equation and the experimental data. It is concluded that the proposed empirical kinetic model from the present study can be used to calculate the nickel dissolution rate of this saprolitic ore using citric acid under atmospheric pressure and the current leaching conditions.

Conclusions

The optimum recovery of nickel (95.6 percent) from an Indonesian saprolite from Sulawesi Island was achieved under leaching conditions of ore particle size of 212-355 microns, citric acid concentration of 1 M, leaching time of 15 days, pulp density of 20 w/v percent, temperature of 40°C and shaker speed of 200 rpm. The experimental data were well interpreted by a shrinking-core model under diffusion control through the product layer. Using the Arrhenius expression, the apparent activation energy for the dissolution of nickel was calculated as 12.38 kJ/mol. The low activation energy is consistent with that for a process controlled by diffusion through a solid product layer. The reaction orders with respect to citric acid concentration, pulp density and ore particle size were determined to be 0.48, 0.27 and 0.32, respectively. The proposed empirical model of the leaching kinetics of this saprolite ore using citric acid under atmospheric pressure can be expressed as:

$$k_d t = 1 - 3(1-x)^{\frac{2}{3}} + 2(1-x) = 7.32 \times 10^{-4} [C_6H_8O_7]^{0.48} (S/L)^{0.27} (r_0)^{0.32} e^{-\frac{12,380}{RT}} t$$

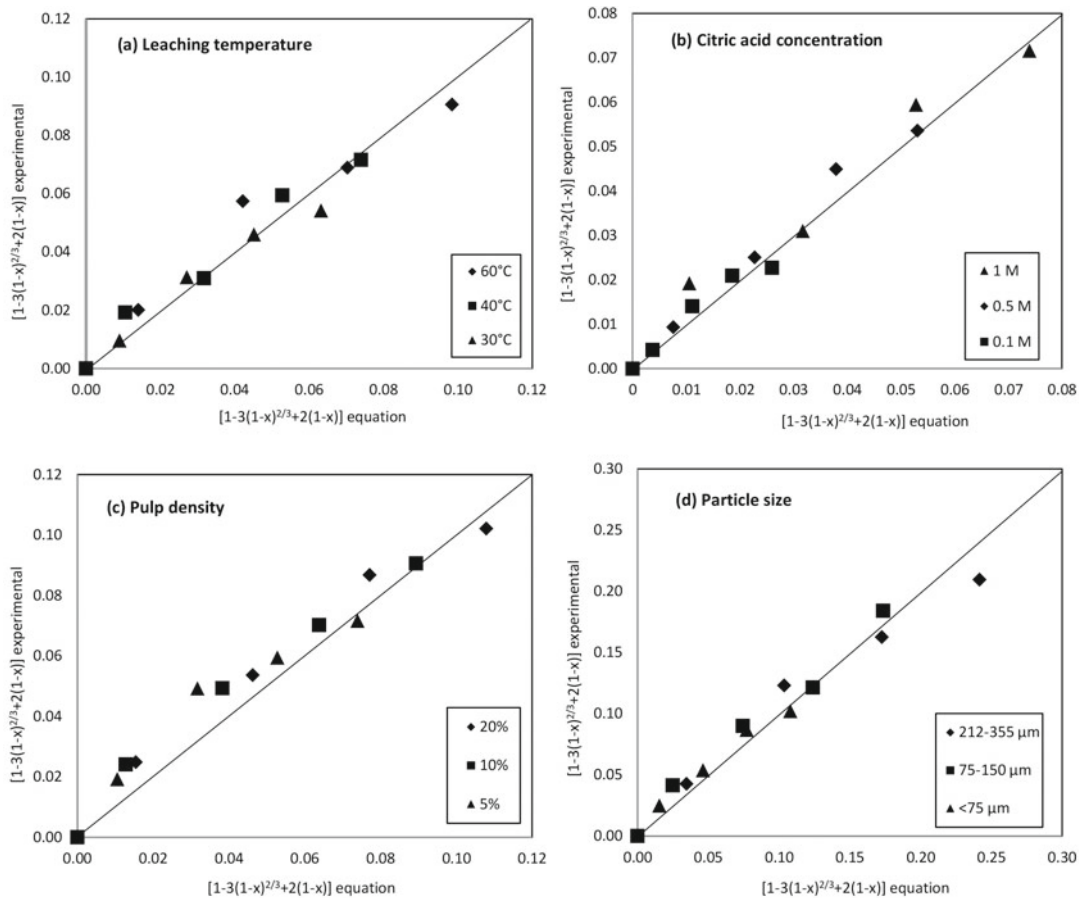


Figure 16 – Validation of the empirical kinetic model for various leaching parameters: (a) leaching temperature (b) citric acid concentration (c) pulp density and (d) particle size.

This mathematical model was verified to be consistent with the observed experimental results.

Acknowledgments

The authors gratefully acknowledge a Grant-in-Aid for Science Research (No. 24246149), a JSPS Kakenhi – Grant-in-Aid for Scientific Research (A) – Grant No. 15H02333, the Japan Society for the Promotion of Science and the Ministry of Education, Culture, Sports, Science and Technology, Japan, for financial and other support and Dr. M. Zaki Mubarak at Bandung Institute of Technology, Indonesia, for support with regards to saprolitic ore samples.

References

Behera, S.K., Panda, P.P., Singh, S., Pradhan, N., Sukla, L.B., and Mishra, B.K., 2011, "Study on reaction mechanism of bioleaching of nickel and cobalt from lateritic chromite overburdens," *International Biodeterioration & Biodegradation*, Vol. 65, pp. 1035-1042.

Fan, R., and Gerson, A.R., 2013, "Mineralogical characterization of Indonesian laterites prior to and post atmospheric leaching," *Hydrometallurgy*, Vol. 134-135, pp. 102-109.

Gharabaghi, M., Irannajad, M., and Noaparast, M., 2010, "A review of the beneficiation of calcareous phosphate ores using organic acid leaching," *Hydrometallurgy*, Vol. 103, pp. 96-107.

Guo, X., Li, D., Park, K.H., Tian, Q., and Wu, Z., 2009, "Leaching behavior of metals from a limonitic nickel laterite using a sulfation-roasting-leaching process," *Hydrometallurgy*, Vol. 99, pp. 144-150.

Habashi, F., 1969, *Principles of Extractive Metallurgy*, General Principles, Vol. 1, Gordon and Breach, New York, 413 pp.

Hou, X., Xiao, L., Gao, C., Zhang, Q., and Zeng, L., 2010, "Kinetics of leaching

selenium from Ni-Mo ore smelter dust using sodium chlorate in a mixture of hydrochloric and sulfuric acids," *Hydrometallurgy*, Vol. 104, pp. 76-80.

Levenspiel, O., 1999, *Chemical Reaction Engineering*, 2nd Edition, John Wiley, 684 pp.

Liu, K., Chen, Q., Yin, Z., Hu, H., and Ding, Z., 2012, "Kinetics of leaching of a Chinese laterite containing maghemite and magnetite in sulfuric acid solutions," *Hydrometallurgy*, Vol. 125-126, pp. 125-136.

Lu, J., Liu, S., Du, W., Pan, F., and Yang, S., 2013, "The effect of sodium sulphate on the hydrogen reduction process of nickel laterite ore," *Minerals Engineering*, Vol. 49, pp. 154-164.

Luo, W., Feng, Q., Ou, L., Zhang, G., and Chen, Y., 2010, "Kinetics of saprolitic laterite leaching by sulphuric acid at atmospheric pressure," *Minerals Engineering*, Vol. 23, pp. 458-462.

McDonald, R.G., and Whittington, B.I., 2008, "Atmospheric acid leaching of nickel laterites review. Part II. Chloride and bio-technologies," *Hydrometallurgy*, Vol. 91, pp. 56-69.

Merchant Research and Consulting Ltd, 2014, "Nickel: 2014 Market Review and Forecast," January, 57 pp.

Mubarak, M.Z., Astuti, W., and Chaerun, S.K., 2011, "Leaching behavior of nickel from Indonesian laterite ore in some organic acids," *Proceedings of the International Mineral Processing Symposium*, Turkey.

Romankiv, L.T., and Bruyn, D., 1964, *Unit Process in Hydrometallurgy*, M.E. Wadsworth and F.T. Davis, eds., Academic Press, New York, p. 62.

Sohn, H.Y., and Wadsworth, M.E., 1979, *Rate Process of Extractive Metallurgy*, Plenum Press, New York and London, 472 pp.

Sufriadin, Arifudin Idrus, Subagyo Pramujoyo, I. Wayan Warmada, and Akira Imai, 2011, "Study on mineralogy and chemistry of the saprolitic nickel ores from Soroako, Sulawesi, Indonesia: Implication for the laterite ore processing," *J. SE. Asian Appl. Geol.*, Jan-Jun 2011, Vol. 3, No. 1, pp. 23-33.

Tang, J.A., and Valix, M., 2006, "Leaching of low grade limonite and nontronite ores by fungi metabolic acids," *Minerals Engineering*, Vol. 19, pp. 1274-1279.

Tzeferis, P.G., and Agatzini-Leonardou, S., 1994, "Leaching of nickel and iron from Greek non-sulphide nickeliferrous ores by organic acid," *Hydrometallurgy*, Vol. 36, No. 3, pp. 345-360.

Veglio, F., Trifoni, M., Pagnanelli, F., and Toro, L., 2001, "Shrinking core model with variable activation energy: A kinetic model of manganiferous ore leaching with sulfuric acid and lactose," *Hydrometallurgy*, Vol. 60, pp. 167-179.